

Turbulent Thermal Diffusion: A Way to Concentrate Dust in Protoplanetary Discs

Alexander Hubbard,^{1*}

¹*Department of Astrophysics, American Museum of Natural History, New York, NY 10024-5192, USA*

Accepted XXX. Received YYY; in original form ZZZ

ABSTRACT

Turbulence acting on mixes of gas and particles generally evenly diffuses the latter through the former. However, in the presence of background gas temperature gradients a phenomenon known as turbulent thermal diffusion appears as a particle drift velocity (rather than a diffusive term). This process moves particles from hot regions to cold ones. We rederive turbulent thermal diffusion using astrophysical language and demonstrate that it could play a major role in protoplanetary discs by concentrating particles by factors of tens. Such a concentration would set the stage for collective behavior such as the streaming instability and hence planetesimal formation.

Key words: hydrodynamics – turbulence – planets and satellites: atmospheres – planets and satellites: formation

1 INTRODUCTION

In this paper we examine a phenomenon in which turbulence transports particles down temperature gradients: turbulent thermal diffusion (TTD), which was originally recognized by [Elperin et al. \(1996\)](#) and subsequently verified in laboratory experiments ([Eidelman et al. 2004, 2006](#)). The TTD has astrophysical consequences. For example, planetary atmospheres have vertical varying temperature profiles which play a major role in the formation of hazes and clouds via condensation ([Ackerman & Marley 2001](#)). The TTD is known to trap particles in such temperature bands in the Earth’s atmosphere ([Sofiev et al. 2009](#)); and has been hypothesized to do so elsewhere in the Solar System ([Elperin et al. 1997](#)).

Protoplanetary discs also have temperatures that vary strongly on both global and local scales, as has been seen in observations of protoplanetary disks, and as has been demonstrated by laboratory examinations of meteorites ([Hewins & Radomsky 1990](#); [D’Alessio et al. 2005](#)). While models of the background disk temperature, including both heating by irradiation from the central star and heating from accretion power, predict temperatures that scale as the square-root of the orbital position, numerical simulations of turbulent accretion disks that focused on the gas’s thermal behavior have seen order unity temperature fluctuations on far smaller, scale-height length scales ([McNally et al. 2014](#)). Indeed, large local temperature gradients have many possible sources, including shadowing ([Dullemond 2000](#)), and transitional regions such as the boundary between magnetically active and magnetically dead regions ([Zhu et al. 2009](#)), evaporation fronts ([Dullemond & Monnier 2010](#)), or the edges of planet-opened gaps ([Turner et al. 2012](#)). A natural question that arises is to what extent these global and local

temperature variations influence the nature and dynamics of solids in such disks, and thereby also influence planet formation. In particular, the TTD could play a significant role in the transport and concentration of particles in discs, similarly to how it acts in planetary atmospheres.

The smaller spatial scale temperature fluctuations that occurred in our own Solar Nebula, and presumably occur in other protoplanetary disks, have consequences beyond the TTD, i.e. the thermal processing of solid material, (e.g. chondrule formation, [Hewins 1997](#)). Sufficient heating will cause fluffy particles to compactify, reducing its effective surface area and thereby reducing (although not eliminating) its interaction with the gas. This accelerates the rate with which the compactified particles settle or drift radially ([Hubbard & Ebel 2014](#)). In addition, temperature fluctuations can also move particles more directly such as through photophoresis, which has been invoked to explain Solar Nebula phenomena such as the outwards radial transport of CAIs ([Ehrenhaft 1918](#); [Wurm & Haack 2009](#)). In an optically thick disk, a particle radiatively exchanges thermal information with a shell an optical depth in radius. Different sides of a particle can therefore see gas at different temperatures, which sets up temperature gradients through the particle. The difference in temperature across the particle’s surface cause gas molecules to recoil more violently from the hotter side, pushing the particles from hot regions to cold, with consequences for protoplanetary disks ([McNally & Hubbard 2015](#)). However, photophoresis depends on the radiative flux, as so requires a high background temperature in addition to a strong temperature gradient.

In this paper we focus only on the TTD, where, as the name suggests, it is turbulence rather than the radiation field that plays the central role. Our purpose is two-fold: firstly, we introduce the TTD to the astrophysics community and develop it in a more familiar language. In doing so we write the conditions for the TTD to apply

* E-mail: ahubbard@amnh.org

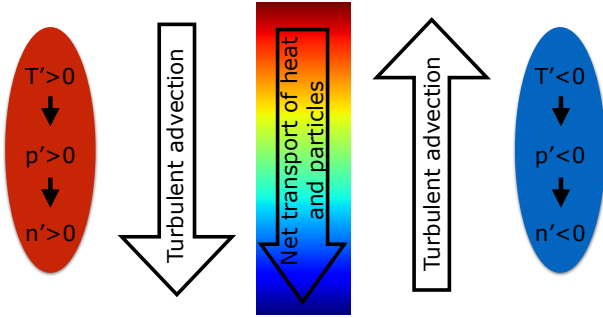


Figure 1. Cartoon of the TTD. Turbulent motions moving down (up) a background temperature gradient drags gas to colder (warmer) regions. The warmer (colder) turbulently advected gas has higher (lower) pressure than the ambient gas. The higher (lower) pressure turbulently advected gas concentrates (disperses) particles, resulting in net particle transport.

in terms sufficiently general that they can be easily adapted to systems where the transport of solids by gas are important, including exoplanetary and brown dwarf atmospheres. Secondly, we explore TTD's consequences for particle transport in protoplanetary disks in particular and show that while background power-law temperature gradients are too weak to support the TTD, cold annuli about a local scale height wide are expected to significantly concentrate millimeter to centimeter scale particles in protoplanetary disks.

2 TURBULENT THERMAL DIFFUSION

As we will quantify, in general, the TTD acts as a first order effect when all of the following are satisfied: (1) the temperature gradient is steeper than the pressure gradient, (2) particles are well, but not perfectly, coupled to the turbulence, and (3) the turbulence is subsonic. The latter two conditions are linked: the better particles are coupled to the turbulence, the more subsonic the turbulence needs to be. Finally, while the TTD can act on very well coupled particles if the turbulence is sufficiently weak, the time scale for it to do so can be prohibitive.

Inertial particles, with finite mass $m_p \gg m$, the mean molecular mass of the gas they are embedded in, drift through the gas even if they are frictionally well coupled. We write the equations for \mathbf{w} , the particle's drift speed through the gas (Equations A6 and A7), as

$$\mathbf{w} \equiv \mathbf{v} - \mathbf{u}, \quad (1)$$

$$\partial_t \mathbf{w} = -\frac{\mathbf{w}}{\tau_s} + \dots, \quad (2)$$

where \mathbf{v} is the particle's velocity, \mathbf{u} the gas velocity at the particle's position, and τ_s the particle's frictional stopping time.

Because even well coupled particles embedded in the gas are too large to feel pressure forces, they drift through the gas up pressure gradients according to

$$\mathbf{w} = \frac{\tau_s}{\rho} \nabla p, \quad (3)$$

where ρ is the gas density. Taking the divergence of Equation (3), we can see that pressure maxima concentrate particles, and indeed

$$n' \simeq t_p \partial_t n' \simeq t_p \nabla \cdot n \mathbf{w} \simeq n \frac{t_p \tau_s}{\rho} \nabla^2 p \propto \frac{n \tau_s t_p}{\rho} \frac{p'}{l_p^2}, \quad (4)$$

where n is the background particle number density, n' the fluctuating particle number density, p' a pressure fluctuation, l_p its length scale and t_p its life time. In the presence of turbulence, there is a fluctuating velocity field \mathbf{u}' which creates a fluctuating pressure field p' which in turn generates a fluctuating particle number density field n' . This n' is the signature of preferential concentration (Maxey 1987; Cuzzi et al. 2001); but in the absence of large scale gas gradients, symmetry means that there is no preferred direction for averaged vector quantities to be aligned with. As a result,

$$\langle n' \mathbf{u}' \rangle \propto \langle p' \mathbf{u}' \rangle = 0, \quad (5)$$

and there is no large scale particle transport.

The presence of a large scale gas temperature gradient strongly alters the situation. The key insight of Elperin et al. (1996) was that for gas in hydrostatic equilibrium, the fluctuating gas density and velocity fields are at most weakly correlated because there is no net turbulent transport of gas mass even in the presence of a gas density gradient; but in the presence of a gas temperature gradient, there is net turbulent transport of heat down the temperature gradient. Therefore, the correlation of \mathbf{u}' and p' can be approximated as (Equation A47):

$$\begin{aligned} \langle p' \mathbf{u}' \rangle &= \left\langle \frac{k_B}{m} (\rho T' + \rho' T) \mathbf{u}' \right\rangle \\ &\simeq \left\langle \frac{\rho k_B T'}{m} \mathbf{u}' \right\rangle \simeq \left\langle \frac{\rho k_B (-t_t \mathbf{u}' \cdot \nabla T)}{m} \mathbf{u}' \right\rangle \neq 0, \end{aligned} \quad (6)$$

where t_t is the turbulent correlation timescale. Invoking Equation (4) we find our expected scaling:

$$\langle n' \mathbf{u}' \rangle \propto n \frac{\tau_s t_p}{l_p^2} \langle p' \mathbf{u}' \rangle \propto -n \frac{\tau_s k_B}{m} \nabla T, \quad (7)$$

where we have used $t_p = t_t$, and $|\mathbf{u}'| \simeq l_p/t_p$ for turbulent fluctuations. Accordingly, Equation (6) implies that turbulence pumps particles from hot regions to cold ones, as sketched in Figure 1. In essence, the TTD acts by having turbulent, small scale pressure gradients generate local clumps of particles, and then having global scale temperature gradients lead to those clumps moving in an ordered fashion.

The temperature fluctuations T' invoked above are not due to local sonic compression but rather to turbulence advecting gas of different temperatures ($T' \simeq -t_t \mathbf{u}' \cdot \nabla T$ for an appropriate turbulent correlation time t_t). This leads to a key aspect of the TTD: $\langle p' \mathbf{u}' \rangle \propto \langle \mathbf{u}'^2 \rangle$, so p' depends on the turbulent speed linearly rather than quadratically as is generally the case (e.g. dynamic pressure and Bernoulli's principle). Because presence of a gas temperature gradient strongly enhances the magnitude of p' , it also leads to enhanced preferential concentration beyond the scope of this paper (Eidelman et al. 2010). While we do not know of any simple calculation showing why the gas avoids relaxation to more modest pressure fluctuations, in Section A9 we further explore the consequences of assuming

$$\frac{p'}{p} \propto \text{Ma}^2, \quad (8)$$

where Ma is the turbulent Mach number. We find that, in that regime, only minor particle transport occurs. Laboratory experiment and atmospheric observations have found strong effects, implying that the approximations in Equation (6) are indeed appropriate and that Equation (8) should not be used (Eidelman et al. 2004; Sofiev et al. 2009).

2.1 Equations of the TTD

We derive the TTD beyond the scaling of Equation (7) in Appendix A. The derivation is highly involved (note the equation numbers referenced), and is not needed to explore its astrophysical consequences, so we limit ourselves to using those results. We therefore quote Equations A44, A61, A62 and A68 to encapsulate the TTD (up to approximations made explicit in Appendix A):

$$\partial_t n + \nabla \cdot \mathbf{F}_n \simeq 0, \quad (9)$$

$$\mathbf{F}_n = n (\mathcal{D} \nabla [\ln \rho - \ln n] + \mathbf{w} + \mathbf{V}_{\text{TTD}}), \quad (10)$$

$$\mathbf{V}_{\text{TTD}} = -\frac{4}{3} C \tau_s \frac{k_B T}{m} \ln \text{St}^{-1} \nabla \ln T, \quad (11)$$

$$\mathbf{w} = \frac{\tau_s}{\rho} \nabla p, \quad (12)$$

where n and \mathbf{F}_n are the particle number densities and fluxes (not normalized to the gas density); τ_s and St are the particle stopping time and Stokes number normalized to the integral scale of the turbulence (Equation A59); ρ , p , T and m are the gas density, pressure, temperature and mean molecular mass; \mathcal{D} is the turbulent diffusion coefficient; and C is a coefficient of order unity. The main difference between Equation (7) and Equation (11), the factor of $\ln \text{St}^{-1}$, is due to the fact that turbulence has a power spectrum, rather than specific values for its velocity, length scale and time scale.

Note that our analysis has been performed in the $\text{St} \ll 1$ limit (i.e. particle frictional stopping times much shorter than turbulent correlation times) to allow scale separation between the dust stopping time τ_s and the turbulent correlation time scales. We have also assumed an approximately adiabatic equation of state, with thermal relaxation negligible on turbulent advective time scales. Thermal relaxation on timescales comparable with the turbulent advective time scale would add a prefactor below unity to Equation (A50), reducing our estimate for turbulent thermal fluctuations; while thermal relaxation on time scale far shorter than the turbulent time scale would eliminate the effect.

\mathbf{V}_{TTD} , the particle turbulent thermal diffusion velocity, is the focus of this paper. Note that both \mathbf{w} and \mathbf{V}_{TTD} are proportional to τ_s , but $\mathbf{w} \neq 0$ requires the existence of a large scale pressure gradient, while $\mathbf{V}_{\text{TTD}} \neq 0$ relies on the existence of a large scale temperature gradient. For an ideal gas, those gradients often are, but need not be, related; and even when both exist, they need not be aligned or anti-aligned, so the two velocities can act in concert, or in opposition. Note also that the form for \mathbf{V}_{TTD} in Equation (11) does not make reference to the turbulent velocity scales, which have cancelled out. As discussed in Section A7, our analysis is performed in the limit $n'/n \ll 1$, which implies that $V_{\text{TTD}} \ll u_0$, the turbulent velocity at the integral scale. When that constraint is violated Equation (11) cannot be used, but the fluctuating particle number density field n'/n is not small and must therefore nonetheless be treated with care.

In general we can have both large scale temperature and pressure gradients, and so need to consider both \mathbf{V}_{TTD} and \mathbf{w} . For the TTD to be a first order effect, we need $|\mathbf{V}_{\text{TTD}}| \gtrsim |\mathbf{w}|$. We therefore determine the conditions for the TTD to be important in Section 2.2 and derive the TTD in the special case of $\mathbf{w} \sim 0$ in Section 2.3.

2.2 General case

From Equations (11) and (12) we have

$$\mathbf{V}_{\text{TTD}} = -\frac{4}{3} \frac{C \tau_s k_B T}{m} \ln \text{St}^{-1} \frac{\hat{\mathbf{e}}_T}{L_T}, \quad (13)$$

$$\mathbf{w} = \frac{\tau_s}{\rho} p \frac{\hat{\mathbf{e}}_p}{L_p} = \frac{\tau_s k_B T}{m} \frac{\hat{\mathbf{e}}_p}{L_p}, \quad (14)$$

where $\hat{\mathbf{e}}_p$ and $\hat{\mathbf{e}}_T$ are the directions of the pressure and temperature gradients while L_p and L_T are the lengthscales over which the pressure and temperature vary:

$$L_p = |\nabla \ln p|^{-1}, \quad (15)$$

$$L_T = |\nabla \ln T|^{-1}. \quad (16)$$

We can write two alternative conditions for the TTD to be an important player:

$$|\mathbf{V}_{\text{TTD}}| \gtrsim |\mathbf{w}|, \quad (17)$$

$$|\mathbf{V}_{\text{TTD}}^2| \gtrsim |\mathbf{V}_{\text{TTD}} \cdot \mathbf{w}|, \quad (18)$$

where the first condition only compares the magnitudes of the two velocities and the second also considers the degree of alignment.

Using Equations (13) and (14), Equations (17) and (18) become:

$$\frac{4}{3} \frac{L_p}{L_T} C \ln \text{St}^{-1} \gtrsim 1, \quad (19)$$

$$\frac{4}{3} \frac{L_p}{L_T} C \ln \text{St}^{-1} \gtrsim |\hat{\mathbf{e}}_p \cdot \hat{\mathbf{e}}_T|. \quad (20)$$

In what follows we will consider only the more restrictive Equation (19).

2.3 Isobaric case

If Equation (19) is very well satisfied, then we can neglect the particle drift velocity \mathbf{w} and note that $L_p \gg L_T$, (i.e. the system is effectively isobaric). This allows us to simplify

$$\nabla \ln \rho = \nabla \ln p - \nabla \ln T \simeq -\nabla \ln T. \quad (21)$$

Using that simplification, Equations (10) and (11) become

$$\mathbf{F}_n = -n \mathcal{D} (\nabla \ln n + \alpha \nabla \ln T), \quad (22)$$

$$\alpha \equiv 1 + \frac{4C}{3\mathcal{D}} \tau_s \frac{k_B T}{m} \ln \text{St}^{-1}, \quad (23)$$

$$\mathbf{V}_{\text{TTD}} = -(\alpha - 1) \mathcal{D} \nabla \ln T, \quad (24)$$

where $(\alpha - 1)$ measures the relative strength of turbulent diffusion and turbulent thermal diffusion. We use the definition in Equation (23) to follow existing literature (e.g. Eidelman et al. 2004); and note that it is the natural parameter for experiments where the gas temperature and the particle number density are easy to measure directly, but the gas density and particle concentration, are not.

3 CONSEQUENCES OF TURBULENT THERMAL DIFFUSION

3.1 Isobaric equilibrium distribution

As has been previously calculated (e.g. Eidelman et al. 2006), we can use Equation (22) to find that the steady state particle distribution ($\mathbf{F}_n = 0$):

$$n \propto T^{-\alpha} \propto \rho^\alpha. \quad (25)$$

For non-inertial particles perfectly coupled to the gas, $\tau_s = 0$, so $\alpha = 1$ and $n \propto \rho$: as expected, turbulent mixing drives the system to a uniform particle concentration. For inertial particles, $\tau_s > 0$, $\alpha > 1$,

$$\frac{n}{\rho} \propto T^{-(\alpha-1)}, \quad (26)$$

and colder regions concentrate particles.

Experiments have found values up to about $\alpha \simeq 2.7$ (Eidelman et al. 2006) while observations of aerosols in the troposphere indicate that $\alpha > 20$ occurs in nature (Sofiev et al. 2009). Note that our analysis assumes that the dust fluid density is always much less than that of the gas, so that any drag the dust exerts on the gas can be neglected. Large values of α could imply local concentrations of dust large enough exceed that limit. Our analysis can no longer be applied once such conditions occur, but those conditions would also allow other processes to dominate (e.g. Johansen et al. 2007). In situations where the background dust fluid density is too low to backreact on the gas, but the TTD would generate concentrations of dust sufficiently dense to backreact on the gas, the TTD can be invoked as a trigger for processes such as the streaming instability.

3.2 Conditions for relevance

While the parameter C has not yet been determined, and likely varies depending on the nature of the turbulence, we expect $C < 1$ and Zilitinkevich et al. (2007) suggests $C \sim 0.3$. In that case, Equation (19) becomes

$$\text{St} \lesssim e^{-2.5L_T/L_p}. \quad (27)$$

The shorter the temperature length scale is compared to the pressure length scale, the larger the particles can be and still get transported by the TTD. This is important because the TTD transports larger particles faster, and larger particles are more likely to engage in collection behavior such as the streaming instability. In astrophysical cases of interest such as planetary atmospheres in hydrostatic equilibrium or protoplanetary disk midplanes, temperature, density and pressure generally vary in the same direction and on comparable length scales in the absence of specific phenomena driving more localized fluctuations. From Equation (27) we can see that the limits on St depend very strongly on L_T/L_p , and so in general, TTD can overcome pressure based particle drift only in the limit of very small St , or in the presence of local phenomena which force $L_T \ll L_p$ (i.e. the isobaric limit).

However, the limit of very small St means particles which are extremely well coupled to the gas and so generally well mixed by turbulence. We define the Mach number of the turbulence as

$$\text{Ma} \equiv \frac{u_0^2}{c_s^2} = \frac{u_0^2 \rho}{\gamma p} = \frac{m u_0^2}{\gamma k_B T}, \quad (28)$$

and use that along with Equation (A56) to rewrite Equation (23) as

$$\alpha - 1 = \frac{4C}{u_0^2} \frac{\tau_s}{t_0} \frac{k_B T}{m} \ln \text{St}^{-1} = \frac{8C}{\gamma} \frac{\text{St}}{\text{Ma}^2} \ln \text{St}^{-1}. \quad (29)$$

If Equation (27) is to be satisfied by decreasing St , then the TTD will have an effect only for weak turbulence ($\text{Ma}^2 < \text{St}$).

TTD therefore generally applies to astrophysical systems with temperature fluctuations on length scales that are simultaneously much larger than the turbulent length scales, and much smaller than the length scales associated with pressure ($\ell_0 \ll L_T \ll L_p$). When the TTD applies, in practice it concentrates and disperses particles with $1 \gg \text{St} > \text{Ma}^2$.

4 TEMPERATURE GRADIENTS IN PROTOPLANETARY DISKS

4.1 Global temperature gradients

Turbulent thermal diffusion has been invoked to explain aerosol concentrations in the Earth's tropopause, and could similarly be applied to exoplanetary and brown dwarf atmospheres, including both vertical and horizontal temperature stratification. Here we explore the TTD's consequences for protoplanetary disk midplanes, noting that protoplanetary disks are slightly awkward because anticipated parameters only marginally satisfy the assumptions built into our analytical analysis. We assume the scalings of a Hayashi Minimum Mass Solar Nebula (MMSN, Hayashi 1981). Note that discs are generally assumed to be statistically symmetric about the midplane, and are azimuthally periodic, so near the midplane the vertical/azimuthal plane is homogenous and can be averaged over, leaving only the radial variations.

Background disk temperature gradients are shallow power-laws, occurring on orbital length scales, and as we calculate next, are not expected to support significant TTD. In a Hayashi MMSN, the midplane temperature and pressure scale with orbital position R as:

$$T \propto R^{-1/2}, \quad (30)$$

$$p \propto R^{-13/4}, \quad (31)$$

from which we find

$$L_T = 2R, \quad (32)$$

$$L_p = \frac{4}{13}R. \quad (33)$$

Note that in this case, \mathbf{w} points radially inwards (headwind induced infall, Weidenschilling 1977) while \mathbf{V}_{TTD} points outwards. With those values for the global gradients, Equation (27) is satisfied for

$$\text{St} \lesssim 10^{-7}, \quad (34)$$

i.e. for particles sufficiently coupled to the gas that no meaningful drift occurs regardless. However, for $C = 2/3$ we would have $\text{St} \lesssim 7 \times 10^{-4}$, which begins to be relevant. Even for $C = 0.3$, the TTD can slow headwind induced infall by a few tens of percents: if $\text{St} = 0.01$ then $\mathbf{V}_{\text{TTD}} \sim -0.3 \mathbf{w}$.

4.2 Local, quasi-isobaric temperature gradients

While background protoplanetary disk global temperature gradients are expected to be too weak relative to global pressure gradients for TTD to be a first order effect, protoplanetary disk temperatures are not expected to follow perfect power-laws, but rather are expected to also show strong, localized temperature variations on scales much smaller than the orbital length scale. For example, if the dominant source of heating in a disk is irradiation by the central object, then shadowing can occur: when an annulus of the disk heats, it puffs up, shadowing the disk outside it, which then cools and contracts (Dullemond 2000; Siebenmorgen & Heymann 2012). Similarly, turbulence can generate long lived, quasi-isobaric order-unity temperature, fluctuations on length scales only a few percent of the orbital position (McNally et al. 2014); and boundaries between regions with different chemistry provide highly localized, extremely long lived sharp temperature gradients Zhu et al. (2009); Dullemond & Monnier (2010). We can check the requirements for such local temperature variations to allow the TTD to operate.

For the quasi-isobaric approximations to apply, we need to

satisfy Equation (27) for non-negligible values of St . As noted above, this requires some form of temperature perturbation on top of the expected background power-law of Equation (30). One possible source is turbulent dissipation. Magneto-hydrodynamical turbulence dissipates its energy in quasi-2D structures known as current sheets; and, in protoplanetary disks, these structures can be very thin, hot, and in pressure balance with the exterior. McNally et al. (2014) found order unity temperature variation on length scales only a few percent of the orbital position with negligible associated pressure structures. These structures clearly would satisfy Equation (27) for particles with large enough St to slip through the gas on short time scales.

Another possible way to generate temperature annuli is shadowing (Dullemond 2000; Siebenmorgen & Heymann 2012). In this case, we note that the gas midplane density in a vertically isothermal disk is

$$\rho_0 = \frac{\Sigma}{\sqrt{2\pi}H} = \frac{\Sigma\Omega_K}{\sqrt{2\pi}c_s}, \quad (35)$$

where Σ is the gas surface density, H the pressure scale height and Ω_K the local Keplerian frequency. We also have

$$c_s^2 = \frac{\gamma k_B T}{m}. \quad (36)$$

It follows that the midplane pressure is given by

$$p_0 = \frac{\rho_0 c_s^2}{\gamma} = \sqrt{\frac{k_B T}{2\pi\gamma m}} \Sigma \Omega_K. \quad (37)$$

While the onset of shadowing will have a major impact on the temperature profile, strong Coriolis forces imply that shadowing is not expected to significantly redistribute mass radially. As long as the temperature gradient caused by shadowing obeys $L_T^{-1} \gg \partial_R \ln \Sigma \sim R^{-1}$ we can therefore use Equations (15), (16) and (37) to approximate

$$L_p \sim 2L_T. \quad (38)$$

In that case Equation (27) would require $St \lesssim 0.24$. That upper limit is safely above values associated with the fragmentation or bouncing barriers, and is safely large enough for the streaming instability to act (Zsom et al. 2010; Carrera et al. 2015).

5 QUASI-ISOBARIC PROTOPLANETARY TEST CASE

The potential range of parameters for protoplanetary disks is too large to fully analyse here. Instead, we derive a test case that shows that there are plausible regions of parameter space in which the TTD would significantly concentrate dust in protoplanetary disks. The constraints we use to choose the test-case parameters can be used to check other models for the importance of the TTD.

5.1 Quasi-isobaric particle concentration

In the common α -disk model, protoplanetary disks are assumed to accrete due to turbulent stresses, with a corresponding viscosity $\alpha_{SS} c_s H$, where α_{SS} represents the Shakura-Sunyaev α (Shakura & Sunyaev 1973), not to be confused with the α of Equation (23). We assume here that the turbulent viscosity $\alpha_{SS} c_s H$ is approximately equal to the turbulent diffusivity \mathcal{D} , i.e. a Schmidt number $Sc \sim 1$ (Johansen et al. 2006). The time scale of the turbulence driven by orbital shear is also generally assumed to lie around Ω_K^{-1} (Fromang & Papaloizou 2006). It follows that

$$u_0 \sim \sqrt{\alpha_{SS} c_s}, \quad (39)$$

and hence

$$Ma^2 \sim \alpha_{SS}. \quad (40)$$

Accordingly, Equation (29) becomes

$$\alpha - 1 \sim 1.7 \frac{St}{\alpha_{SS}} \ln St^{-1}, \quad (41)$$

where we have assumed $C = 0.3$ and $\gamma = 1.4$. We can see that significant TTD effects are expected only for $St > \alpha_{SS}$, and that Jacquet et al. (2012)'s parameter $S \equiv St/\alpha_{SS}$ which measure dust transport through gas is very relevant here as well.

Our current understanding of planet formation has difficulties in growing grains with $St \sim 10^{-3}$. Turbulently driven collisions are expected to be at best growth neutral, and often destructive for such grains (Zsom et al. 2010). While the precise size at which collisional growth fails is uncertain, our current picture is that once grains grow large enough ($St \sim 10^{-2}$), collective dust-gas instabilities such as the streaming instability (SI, Johansen et al. 2007) take hold, collecting dust into gravitationally unstable clumps which collapse, forming planetesimals directly. However, this leaves us with a clear dust size gap between the end collisional growth and the triggering of the SI. One further difficulty for the SI is that it requires background dust concentrations that are significantly super-solar, and the degree of metallicity enhancement over solar needed is strongly St dependent. Indeed, Carrera et al. (2015) found that the smallest grains which can trigger the SI have $St \sim 3 \times 10^{-3}$; and that requires a background super-solar dust concentration of about a factor of 5 outside of the water ice line, and about a factor of 15 inside of it. The TTD provides a possible route to generating those super-solar dust concentrations.

The bouncing barrier is expected to occur for particles colliding at approximately $0.1 - 1 \text{ cm s}^{-1}$ and the fragmentation barrier for particles colliding at around 100 cm s^{-1} (Güttler et al. 2010). Turbulently induced collisions have a range of possible speeds however, so particles with characteristic collision speeds that lie between the bouncing and fragmentation barriers are expected to grow slowly through rare collisions at the low end of the speed distribution (Windmark et al. 2012). This leads to a pile up in grain size as growth becomes ever less efficient. We assume particles with $St = 3 \times 10^{-3}$ (the smallest which can trigger the SI, Carrera et al. 2015) and $\alpha_{SS} = 10^{-3}$. Disk thermal speeds in regions of terrestrial planet formation are of order $c_s = 10^5 \text{ cm s}^{-1}$, and expected turbulent dust-dust collision speeds are of order (Hubbard 2013):

$$v_{\text{collision}} \sim 0.25 \sqrt{St \alpha_{SS} c_s} \sim 40 \text{ cm s}^{-1}. \quad (42)$$

This is large enough to lead to bouncing, but likely not fragmentation, and so lies in the regime associated with a size pile up.

For $St = 3 \times 10^{-3}$ and $\alpha_{SS} = 10^{-3}$, Equation (41) estimates $\alpha \sim 30.6$, which through Equation (25) would imply extreme concentrations of particles in cold regions through the TTD. Indeed, a temperature perturbation with amplitude $f_T T$, over a length ℓ_T has a corresponding $L_T = \ell_T / f_T$; so $f_T = 0.2$, $\ell_T = 0.6H$ satisfies $L_T = 3H \simeq 0.1R \ll R$, and stronger temperature gradients, at quasi-constant pressure, have been seen in simulations of MHD turbulence in protoplanetary disks (McNally et al. 2014). With those values, Equation (26) implies a particle concentration by a factor of

$$T^{\alpha-1} \simeq (1 + f_T)^{\alpha-1} \simeq (1 + 0.2)^{30.6-1} \simeq 221. \quad (43)$$

This is easily enough to have strong effects on the behavior of dust in protoplanetary disks, and so the TTD could act as a trigger for

the SI. However these values of St , α_{SS} , f_T and ℓ_T run into the limits of our analysis.

5.2 Test case limitations

Note that Equation (39) also implies

$$\ell_0 \simeq \sqrt{\alpha_{SS}} H, \quad (44)$$

We require $\ell_0 \ll \ell_T$. In this test case, this constraint becomes

$$\ell_0 = 0.03H \ll \ell_T = 0.6H, \quad (45)$$

which is well satisfied, but stronger turbulence (more than an order of magnitude larger α_{SS}) has length scales long enough that for small values of f_T we can only marginally linearize the background temperature field, as was done in Appendix A.

More problematically, from Equation (24) we have

$$|\mathbf{V}_{\text{TTD}}| = (\alpha - 1)\alpha_{SS}c_s \frac{H}{L_T} > \frac{1}{3}(\alpha - 1)\alpha_{SS}c_s. \quad (46)$$

For $St = 3 \times 10^{-3}$ and $\alpha_{SS} = 10^{-3}$, this becomes

$$|\mathbf{V}_{\text{TTD}}| \sim 0.01c_s \simeq 0.3u_0, \quad (47)$$

and the requirement $|\mathbf{V}_{\text{TTD}}| \ll u_0$ is only weakly fulfilled. This means that Equation (24) is likely moderately overestimating \mathbf{V}_{TTD} as discussed in Section A7. Because our analysis has \mathbf{V}_{TTD} increasing with particle St , $St \sim 3 \times 10^{-3}$ lies near the upper limit for which our analysis applies when $\alpha_{SS} = 10^{-3}$.

If we are overestimating \mathbf{V}_{TTD} by a factor of two, then we still have $|\mathbf{V}_{\text{TTD}}| > |w|$, but the concentration factor (Equation 43) drops from a factor of 221 to a factor of

$$1.2^{[30.6-1]/2} \simeq 1.2^{14.8} \simeq 15, \quad (48)$$

which is on the edge of triggering the SI inside the water ice line. The timescale for concentration under these conditions is moderate but not negligible. Halving \mathbf{V}_{TTD} we find

$$\frac{\ell_T}{0.5\mathbf{V}_{\text{TTD}}} \sim 20 \text{ Orbits}. \quad (49)$$

However, smaller particles, with lower values of St , will feel the TTD only in the presence of even weaker turbulence, with a correspondingly larger concentration time scale.

5.3 Test case thermal relaxation

A further constraint on this test case is thermal relaxation, in particular any radiative cooling or heating of turbulent parcels of gas. As noted in Section 2.1, if the relaxation time is shorter than the turbulent time, we expect the TTD to be weakened. As long as we have small temperature fluctuations, and are in the optically thick, dense limit, we can approximate radiative cooling as a diffusive process. For an MMSN midplane at $R = 1 \text{ AU}$, we have an approximate thermal diffusion coefficient (McNally et al. 2014):

$$\mu \simeq 4 \times 10^{12} \left(\frac{T}{270 \text{ K}} \right)^3 \text{ cm}^2 \text{ s}^{-1}. \quad (50)$$

The corresponding thermal relaxation time is

$$\frac{\ell_0^2}{\mu} \simeq 6.25 \times 10^7 \text{ s} \left(\frac{T}{270 \text{ K}} \right)^{-3} \simeq 13 \left(\frac{T}{270 \text{ K}} \right)^{-3} \Omega_K^{-1}. \quad (51)$$

As long as the temperature is modest, the time scale is much longer than the turbulent time scale of Ω_K^{-1} , so the largest scale turbulence is insensitive to radiative thermal relaxation. Thermal relaxation will effect smaller eddies farther down the turbulent cascade.

However, this appears in the equation for \mathbf{V}_{TTD} only logarithmically (Equation A57), and so is relatively unimportant.

On the other hand, radiative thermal diffusion is a strong function of temperature, and Equation (51) would seem to limit the TTD to cool regions of the disk. However, the opacity of the gas-dust mixture depends mostly on the abundance of approximately micron-sized dust grains, and at high temperatures those evaporate, dramatically lowering the opacity and moving the system into the optically thin limit. Further, in regions with low gas density, the gas and dust temperatures can decouple, making radiative cooling even less efficient. Those effects would make Equation (51) a significant underestimate for the thermal relaxation time at much higher temperatures. We therefore expect the TTD to be effective in cool regions (unlike photophoresis, McNally & Hubbard 2015), and possibly at very high temperatures (e.g. chondrule formation) in low density regions, but not in warm, high density and opacity regions.

5.4 Other dust and disc parameters

As disc parameters diverge from the ones in Section 5 the situation gets less clear. Larger values of α_{SS} at constant St both reduce the strength of the TTD (reducing the ratio St/α_{SS} in Equation 41) and increase the length scale associated with turbulence. This latter would begin to weaken the condition that turbulent length scales be much shorter than temperature length scales. Weaker values of α_{SS} would reduce the turbulent speed, resulted in ever more severe overestimates of \mathbf{V}_{TTD} (Equation 46 and subsequent discussion) and longer concentration time scales. Thermal relaxation also becomes more pronounced for smaller values of α_{SS} and their corresponding smaller length scales.

Weaker turbulence than our test case, or larger particles (higher St values) constrains the upper limit on \mathbf{V}_{TTD} and the concentration time scale; while stronger turbulence threatens the scale separation between background and turbulent fields. Nonetheless, it is clear that the presence of scale-height-scaled temperature fluctuations in turbulent protoplanetary disks should generally result in significant concentration of particles with $St \gtrsim \alpha_{SS}$ on moderate time scales. Laboratory or numerical studies will be needed to make precise estimations of the effectiveness of the TTD in protoplanetary disks in practice.

6 CONCLUSIONS

We have adapted analysis of turbulent thermal diffusion to a form more useful for astronomy. The TTD is a process where the combination of turbulent and a background pressure gradient act to pump inertial particles from hot regions to cold ones, and it can lead to large particle concentrations in the latter (Elperin et al. 1996). As such, it acts similarly to the well known concentration of particles in high pressure regions; with the significant difference that temperature, unlike pressure, is not an inherently dynamical parameter (although it is usually strongly correlated with dynamical parameters).

While the TTD has already been considered in the context of planetary atmospheres (Sofiev et al. 2009), we also show that it is expected to act in protoplanetary disks that have \sim scale height wide radial temperature banding, concentrating $St \sim 10^{-3}$ particles in the cold bands by factors of tens. While such a degree of concentration would push our analysis outside of its strict region of applicability, it would be a sufficient metallicity enhancement

to allow the streaming instability to proceed. This suggests that if cold bands are common in protoplanetary disks, they would allow the TTD to act to trigger the SI, and hence would be natural regions of planetesimal formation. Possible sources for such cold annuli include disc self-shadowing and localized turbulent dissipation (Dullemond 2000; Siebenmorgen & Heymann 2012; McNally et al. 2014). Shadowing and turbulent dissipation are not expected to be stationary for disk evolution time scales, but chemical boundaries, including ionization and evaporation fronts, could be, and would also drive steep temperature gradients (Zhu et al. 2009; Dullemond & Monnier 2010). This adds to the already significant interest in such regions as possible places for planet formation (Lyra & Mac Low 2012).

The effects of TTD can be implemented in numerical simulations and theory as an ad-hoc velocity V_{TTD} , but theoretical estimates are only approximate and factors of a few in α have a large impact on the concentration of particles (Equations 25, 43 and 48). Implementing TTD into numerical simulations directly will be difficult, and efforts to date have barely been able to detect the effect (Haugen et al. 2012). Capturing the TTD requires a large dynamical range between the scale of the temperature variation and the scale of the turbulence, and a further large dynamical range between the integral scale of the turbulence and the scale of the turbulence which has the same correlation time as the particle's frictional stopping time. Further, strong effects are only expected in low Mach number turbulence, but depend on gas compressibility, forcing sound waves to be fully captured.

Laboratory experiments can and have constrained V_{TTD} in the Stokes drag regime appropriate for planetary atmospheres (Eidelman et al. 2004, 2006); but probing the Epstein drag regime, where particle sizes are smaller than the gas molecular mean free path, appropriate for protoplanetary disks would require extremely fine particles in a very dilute gas. Nonetheless, this is the most promising avenue for constraining the numerical factors such as C .

ACKNOWLEDGEMENTS

This paper would not have been written without the past efforts of Nathan Kleeorin and Igor Rogachevskii to explain the turbulent thermal diffusion process. The research leading to these results received funding from NASA OSS grant NNX14AJ56G.

REFERENCES

- Ackerman A. S., Marley M. S., 2001, *ApJ*, **556**, 872
 Carrera D., Johansen A., Davies M. B., 2015, *A&A*, **579**, A43
 Cuzzi J. N., Hogan R. C., Paque J. M., Dobrovolskis A. R., 2001, *ApJ*, **546**, 496
 D'Alessio P., Calvet N., Woolum D. S., 2005, in Krot A. N., Scott E. R. D., Reipurth B., eds, *Astronomical Society of the Pacific Conference Series* Vol. 341, *Chondrites and the Protoplanetary Disk*. p. 353
 Dullemond C. P., 2000, *A&A*, **361**, L17
 Dullemond C. P., Monnier J. D., 2010, *ARA&A*, **48**, 205
 Ehrenhaft F., 1918, *Annalen der Physik*, **361**, 81
 Eidelman A., Elperin T., Kleeorin N., Krein A., Rogachevskii I., Buchholz J., Grünefeld G., 2004, *Nonlinear Processes in Geophysics*, **11**, 343
 Eidelman A., Elperin T., Kleeorin N., Rogachevskii I., Sapir-Katiraie I., 2006, *Experiments in Fluids*, **40**, 744
 Eidelman A., Elperin T., Kleeorin N., Melnik B., Rogachevskii I., 2010, *Phys. Rev. E*, **81**, 056313
 Elperin T., Kleeorin N., Rogachevskii I., 1996, *Physical Review Letters*, **76**, 224

- Elperin T., Kleeorin N., Podolak M., Rogachevskii I., 1997, *Planet. Space Sci.*, **45**, 923
 Fromang S., Papaloizou J., 2006, *A&A*, **452**, 751
 Güttler C., Blum J., Zsom A., Ormel C. W., Dullemond C. P., 2010, *A&A*, **513**, A56
 Haugen N. E. L., Kleeorin N., Rogachevskii I., Brandenburg A., 2012, *Physics of Fluids*, **24**, 075106
 Hayashi C., 1981, *Progress of Theoretical Physics Supplement*, **70**, 35
 Hewins R. H., 1997, *Annual Review of Earth and Planetary Sciences*, **25**, 61
 Hewins R. H., Radomsky P. M., 1990, *Meteoritics*, **25**, 309
 Hubbard A., 2013, *MNRAS*, **432**, 1274
 Hubbard A., Ebel D. S., 2014, *Icarus*, **237**, 84
 Jacquet E., Gounelle M., Fromang S., 2012, *Icarus*, **220**, 162
 Johansen A., Klahr H., Mee A. J., 2006, *MNRAS*, **370**, L71
 Johansen A., Oishi J. S., Mac Low M.-M., Klahr H., Henning T., Youdin A., 2007, *Nature*, **448**, 1022
 Lyra W., Mac Low M.-M., 2012, *ApJ*, **756**, 62
 Maxey M. R., 1987, *Journal of Fluid Mechanics*, **174**, 441
 McNally C. P., Hubbard A., 2015, preprint, ([arXiv:1510.03427](https://arxiv.org/abs/1510.03427))
 McNally C. P., Hubbard A., Yang C.-C., Mac Low M.-M., 2014, *ApJ*, **791**, 62
 Shakura N. I., Sunyaev R. A., 1973, *A&A*, **24**, 337
 Siebenmorgen R., Heymann F., 2012, *A&A*, **539**, A20
 Sofiev M., Sofieva V., Elperin T., Kleeorin N., Rogachevskii I., Zilitinkevich S. S., 2009, *Journal of Geophysical Research (Atmospheres)*, **114**, 18209
 Turner N. J., Choukroun M., Castillo-Rogez J., Bryden G., 2012, *ApJ*, **748**, 92
 Weidenschilling S. J., 1977, *MNRAS*, **180**, 57
 Windmark F., Birnstiel T., Ormel C. W., Dullemond C. P., 2012, *A&A*, **544**, L16
 Wurm G., Haack H., 2009, *Meteoritics and Planetary Science*, **44**, 689
 Zhu Z., Hartmann L., Gammie C., McKinney J. C., 2009, *ApJ*, **701**, 620
 Zilitinkevich S. S., Elperin T., Kleeorin N., Rogachevskii I., 2007, *Boundary-Layer Meteorology*, **125**, 167
 Zsom A., Ormel C. W., Güttler C., Blum J., Dullemond C. P., 2010, *A&A*, **513**, A57

APPENDIX A: DERIVATION OF TURBULENT THERMAL DIFFUSION

A1 Equations for Gas and Solids

We here derive in exhaustive detail the equations for turbulent particle transport equations in general, and turbulent thermal diffusion more specifically. We start with the continuity and velocity equations for the gas and particle fluids. The gas density and velocities are denoted ρ and \mathbf{u} while the particle number density and velocity are denoted n and \mathbf{v} . In this paper we assume that the particle fluid has a well defined, single-valued differentiable velocity field. This single-valued velocity approximation breaks down at small scales, which is what allows particle-particle collisions to occur, but the deviation from a well defined velocity field is small.

We assume Kolmogorov turbulence with largest (integral) length and velocity scales ℓ_0 and u_0 . The length scale ℓ_0 is assumed to be much smaller than the length scale associated with global variations in parameters of relevance (such as density), so that those fields can be linearized. We also define the wavenumber $k_0 \equiv \ell_0^{-1}$ and the time scale $t_0 \equiv \ell_0/u_0$; and assume that t_0 is much shorter than global system evolution time scales, so that changes in the background fields can be neglected on turbulent time scales.

For simplicity we assume that all global quantities vary along

the same direction in a linearizable fashion, and we adopt a local cylindrical coordinate system with the z -axis aligned with that direction. We also assume that the xy plane can be meaningfully averaged over (i.e. is periodic, closed, or sufficiently large in extent that boundary terms can be neglected on the time scale of the TTD). In a planetary atmosphere, the general case would have z aligned with altitude, with the temperature varying with height on length scales far shorter than the local pressure scale height, and also far shorter than those associated with latitude or longitude. In a protoplanetary disk, we would generally place ourselves at the midplane, with z aligned with the radial direction, noting that the system is periodic in azimuth and symmetric about the midplane. In this case for us to be able to average over the radial-azimuthal plane we need the turbulent length scale to be short compared not only to the radial gradients, but also compared to the local vertical pressure scale height.

A2 Particle Drift Velocity

Our equations are

$$\partial_t \rho + \nabla \cdot (\rho \mathbf{u}) = 0, \quad (\text{A1})$$

$$\partial_t n + \nabla \cdot (n \mathbf{v}) = 0, \quad (\text{A2})$$

$$\partial_t \mathbf{u} + \mathbf{u} \cdot \nabla \mathbf{u} = -\frac{1}{\rho} \nabla p + \mathbf{g}, \quad (\text{A3})$$

$$\partial_t \mathbf{v} + \mathbf{v} \cdot \nabla \mathbf{v} = -\frac{\mathbf{v} - \mathbf{u}}{\tau_s} + \mathbf{g}, \quad (\text{A4})$$

where p is the gas pressure, \mathbf{g} the acceleration due to gravity (and any other accelerations which effect the gas and particles equivalently) and τ_s is the frictional stopping time for the particles. In this analysis we neglect the possibility of any other forces which act on the gas and particles differently, and we neglect the back reaction of the particle drag on the gas. This last requires that the particle fluid mass density be much less than the gas density, i.e.:

$$m_p n \ll \rho, \quad (\text{A5})$$

where m_p is the mass of a particle.

Defining the drift of the particle fluid through the gas as

$$\mathbf{w} \equiv \mathbf{v} - \mathbf{u} \quad (\text{A6})$$

we can combine Equations A3 and A4 to write

$$\partial_t \mathbf{w} + \mathbf{w} \cdot \nabla (\mathbf{w} + \mathbf{u}) + \mathbf{u} \cdot \nabla \mathbf{w} = -\frac{\mathbf{w}}{\tau_s} + \frac{1}{\rho} \nabla p. \quad (\text{A7})$$

In the case of $\tau_s \ll t_0$, the particles are well coupled to at least the largest scale turbulence. In that case the particles will rapidly reach their terminal velocity and we can approximate both

$$\partial_t \mathbf{w} \simeq 0, \quad (\text{A8})$$

$$\mathbf{w} \propto \tau_s, \quad (\text{A9})$$

so that Equation (A7) becomes

$$\mathbf{w} \simeq \tau_s \left[\frac{1}{\rho} \nabla p - \mathbf{w} \cdot \nabla (\mathbf{w} + \mathbf{u}) - \mathbf{u} \cdot \nabla \mathbf{w} \right], \quad (\text{A10})$$

$$= \frac{\tau_s}{\rho} \nabla p + [\text{terms in } \tau_s^2 \text{ and higher}]. \quad (\text{A11})$$

Note that turbulence involves motions on a range of size and time scales, and Equations (A9) and (A11) neglect the effect of turbulent motions with wave-numbers k high enough that their corresponding time scales $t(k) \lesssim \tau_s$. This is reasonable because turbulent

structures on those size scale do not live long enough to have a significant effect on the particle trajectories, but this places limits on which wavenumbers can be integrated over as will be noted in Section A6.

A3 Mean-field decomposition

As mentioned above, for simplicity we assume that all large scale spatial variations in the background fields are aligned along the r -axis. We perform a mean-field decomposition, with xy averages denoted by overbars and fluctuations denoted by primes:

$$\bar{\rho} \equiv A^{-1} \int_{xy} dx dy \rho, \quad (\text{A12})$$

$$\rho' \equiv \rho - \bar{\rho}, \quad (\text{A13})$$

where

$$A \equiv \int_{xy} dx dy. \quad (\text{A14})$$

Note that the average of a fluctuating quantity is zero:

$$\overline{\rho'} = \overline{[\rho - \bar{\rho}]} = \bar{\rho} - \bar{\rho} = 0. \quad (\text{A15})$$

Using this averaging scheme, only t and z derivatives of averaged quantities survive. Note that this averaging scheme obeys the Reynolds averaging rules, so derivatives commute with averaging.

In the case of a protoplanetary disk annulus at the midplane with the temperature gradient pointing radially, we can adopt a spherical coordinate system with the pole ($\theta = 0$) aligned with the rotation axis of the disk. In that case, at an orbital position R , Equation (A12) becomes

$$\bar{\rho} \equiv \frac{1}{2\pi R \times 2\Delta\theta R} \int_{\theta=\pi/2-\Delta\theta}^{\pi/2+\Delta\theta} R d\theta \int_0^{2\pi} R \sin\theta d\phi \rho. \quad (\text{A16})$$

In Equation (A16), ϕ is the azimuthal angle and we require simultaneously that vertical extent $R\Delta\theta$ be large enough compared to turbulent length scales to average over, and small enough compared to R that curvature can be neglected. In protoplanetary disks we expect turbulent lengthscales to be much smaller than the local scale height, which in turn is expected to be much smaller than the orbital radius, so those conditions can be met.

By horizontally averaging Equation (A1) we find

$$\partial_t \bar{\rho} = -\partial_z (\bar{\rho} \mathbf{u} + \overline{\rho' \mathbf{u}'}), \quad (\text{A17})$$

noting that the net gas mass flux is

$$A^{-1} \int_{xy} dx dy \rho \mathbf{u} = \bar{\rho} \bar{\mathbf{u}} + \overline{\rho' \mathbf{u}'}. \quad (\text{A18})$$

A gas quasi-steady-state with $\partial_t \bar{\rho} \simeq 0$ and no net mass flux in z then satisfies

$$\bar{\rho} \bar{\mathbf{u}} + \overline{\rho' \mathbf{u}'} = 0, \quad (\text{A19})$$

which means that

$$\bar{\mathbf{u}} = -\frac{\overline{\rho' \mathbf{u}'}}{\bar{\rho}} \neq 0 \quad (\text{A20})$$

under this averaging scheme; but also that $\bar{\mathbf{u}}$ is at most second order in the fluctuations.

A4 Gas and particle continuity equations

Splitting Equations (A1) and (A2) into their mean and fluctuating components using Equation (A6) we find

$$\partial_t \bar{\rho} + \nabla \cdot (\bar{\rho} \bar{\mathbf{u}}) + \nabla \cdot (\overline{\rho' \mathbf{u}'}) = 0, \quad (\text{A21})$$

$$\partial_t \bar{\rho}' + \nabla \cdot (\bar{\rho} \mathbf{u}' + \rho' \bar{\mathbf{u}}) + \nabla \cdot (\rho' \mathbf{u}' - \overline{\rho' \mathbf{u}'}) = 0, \quad (\text{A22})$$

$$\partial_t \bar{n} + \nabla \cdot (\bar{n} [\bar{\mathbf{w}} + \bar{\mathbf{u}}]) + \nabla \cdot (\overline{n' \mathbf{w}'} + \overline{n' \mathbf{u}'}) = 0, \quad (\text{A23})$$

$$\begin{aligned} \partial_t \bar{n}' + \nabla \cdot (\bar{n} [\mathbf{w}' + \mathbf{u}']) + \nabla \cdot (n' [\bar{\mathbf{w}} + \bar{\mathbf{u}}]) \\ + \nabla \cdot (n' \mathbf{w}' - \overline{n' \mathbf{w}'}) + \nabla \cdot (n' \mathbf{u}' - \overline{n' \mathbf{u}'}) = 0. \end{aligned} \quad (\text{A24})$$

To proceed we need to use Equations (A22) and (A24) to estimate ρ' and n' for use in Equations (A21) and (A23). We assume that the fluctuations are weak enough that we only need to track Equations (A22) and (A24) to first order in fluctuating quantities, noting from Equation (A20) that $\bar{\mathbf{u}}$ is at most second order in the fluctuations. We further assume that background gradients are weak enough that $\bar{\mathbf{w}}$ can be neglected when estimating n' .

Under those conditions, we can use the first order smoothing approximation (FOSA) to close our system, writing

$$\rho'(t) \simeq \rho'(0) - \int_0^t dt' \nabla \cdot [\bar{\rho}(t') \mathbf{u}'(t')], \quad (\text{A25})$$

$$n'(t) \simeq n'(0) - \int_0^t dt' \nabla \cdot \{ \bar{n}(t') [\mathbf{w}'(t') + \mathbf{u}'(t')] \}. \quad (\text{A26})$$

As long as mean quantities vary slowly compared to turbulent time scales, and noting that the fluctuating quantities vary around zero, we need track the time integrals in Equations (A25) and (A26) only for the turbulent correlation times, finding

$$\rho' \simeq -t_u \nabla \cdot (\bar{\rho} \mathbf{u}'), \quad (\text{A27})$$

$$n' \simeq -t_w \nabla \cdot (\bar{n} \mathbf{w}') - t_u \nabla \cdot (\bar{n} \mathbf{u}'), \quad (\text{A28})$$

for characteristic turbulent time scales t_w and t_u . In what follows we will assume that at every turbulent length scale $t_w = t_u$.

Combining Equations (A21) and (A27) and combining Equations (A23) and (A28), using the fact that mean quantities can only vary in the z direction, we find

$$\partial_t \bar{\rho} + \partial_z (\bar{\rho} \bar{u}_z) - \partial_z \left(t_u u'_z [\bar{\rho} \nabla \cdot \mathbf{u}' + u'_z \partial_z \bar{\rho}] \right) = 0, \quad (\text{A29})$$

$$\begin{aligned} \partial_t \bar{n} + \partial_z (\bar{n} \bar{v}_z) \\ - \partial_z \left(t_u w'_z [\bar{n} \nabla \cdot \mathbf{w}' + w'_z \partial_z \bar{n}] \right) \\ - \partial_z \left(t_u w'_z [\bar{n} \nabla \cdot \mathbf{u}' + u'_z \partial_z \bar{n}] \right) \\ - \partial_z \left(t_u u'_z [\bar{n} \nabla \cdot \mathbf{w}' + w'_z \partial_z \bar{n}] \right) \\ - \partial_z \left(t_u u'_z [\bar{n} \nabla \cdot \mathbf{u}' + u'_z \partial_z \bar{n}] \right) = 0. \end{aligned} \quad (\text{A30})$$

As shown in Equation (A20), $\bar{\mathbf{u}}$ need not be zero, especially in the presence of background density gradients. However, $\bar{\mathbf{u}}$ can be considered an artifact of choosing an averaging scheme which obeys the Reynolds averaging rules rather than a density-weighted average, and fortunately, it can be eliminated from the equations for the dust in favor of turbulent terms: assuming a gas density statistical steady state, we have $\partial_t \bar{\rho} = 0$ and Equation (A29) implies that

$$\bar{\rho} (\bar{u}_z - \overline{u'_z t_u \nabla \cdot \mathbf{u}'}) = \overline{t_u u'_z \partial_z \bar{\rho}}. \quad (\text{A31})$$

Equation (A31) captures the density evolution of turbulent parcels of gas moving across a background gas density gradient.

Combining and rearranging terms in Equation (A30) we arrive

at

$$\begin{aligned} \partial_t \bar{n} + \partial_z (\bar{n} \bar{v}_z) - \partial_z \left(\overline{[t_u w'_z + t_u u'_z + 2t_u w'_z u'_z]} \partial_z \bar{n} \right) \\ - \partial_z \left(\overline{[t_u w'_z + t_u u'_z]} [\nabla \cdot \mathbf{w}' + \nabla \cdot \mathbf{u}'] \bar{n} \right) = 0. \end{aligned} \quad (\text{A32})$$

A5 Ordering

We recall from Equation (A20) that $\bar{\mathbf{u}}$ is at most quadratic in fluctuating quantities. Averaging Equation (A11) we find

$$\bar{\mathbf{w}} \simeq \frac{\bar{\tau}_s}{\bar{\rho}} \nabla \bar{p} + [\text{terms quadratic and higher in fluctuations}]. \quad (\text{A33})$$

Because we have assumed that background quantities vary on long length scales compared to the turbulence, we can approximate

$$\mathbf{w}' \simeq \left(\frac{\tau'_s}{\bar{\rho}} - \frac{\bar{\tau}_s \rho'}{\bar{\rho}^2} \right) \nabla \bar{p} + \frac{\bar{\tau}_s}{\bar{\rho}} \nabla p' \simeq \frac{\bar{\tau}_s}{\bar{\rho}} \nabla p'. \quad (\text{A34})$$

To help identify terms we define

$$\mathcal{D} = \overline{t_u u'^2}, \quad (\text{A35})$$

$$\tilde{\mathcal{D}} = \overline{t_u w'_z + 2t_u w'_z u'_z}, \quad (\text{A36})$$

$$\tilde{w} = \overline{-t_u w'_z \nabla \cdot \mathbf{u}'}, \quad (\text{A37})$$

$$\tilde{u} = \overline{-t_u u'_z \nabla \cdot \mathbf{u}'}, \quad (\text{A38})$$

where \mathcal{D} is the traditional turbulent diffusion coefficient, $\tilde{\mathcal{D}}$ a correction for inertial particles, and \tilde{w} and \tilde{u} are correction terms deriving from our use of a volume (rather than gas density) weighted averaging scheme.

We can now rewrite Equation (A32) as

$$\begin{aligned} \partial_t \bar{n} + \partial_z (\bar{n} [\bar{u}_z + \tilde{u} + \bar{w}_z + \tilde{w}]) - \partial_z (\mathcal{D} \partial_z \bar{n}) \\ - \partial_z (\tilde{\mathcal{D}} \partial_z \bar{n}) - \partial_z \left(\overline{t_u [w'_z + u'_z]} \nabla \cdot \mathbf{w}' \bar{n} \right) \simeq 0. \end{aligned} \quad (\text{A39})$$

Finally, we can use Equation (A31) to write

$$\bar{u}_z + \tilde{u} = \overline{t_u u'^2} \partial_z \ln \bar{\rho} = \mathcal{D} \partial_z \ln \bar{\rho}, \quad (\text{A40})$$

reducing Equation (A39) to

$$\begin{aligned} \partial_t \bar{n} + \partial_z (\bar{n} \mathcal{D} \partial_z [\ln \bar{\rho} - \ln \bar{n}]) + \partial_z (\bar{n} [\bar{w}_z + \tilde{w}]) \\ - \partial_z (\tilde{\mathcal{D}} \partial_z \bar{n}) - \partial_z \left(\overline{t_u [w'_z + u'_z]} \nabla \cdot \mathbf{w}' \bar{n} \right) \simeq 0. \end{aligned} \quad (\text{A41})$$

In Equation (A41), the first two terms are the continuity equation for a passive scalar and the remaining terms are the corrections for particle inertia. Note that, as expected, in the absence of particle inertia the steady state solution obeys $\bar{n} \propto \bar{\rho}$, i.e. a uniform particle concentration.

Turbulence with a wavenumber k has an associated gas velocity $u(k)$. As long as the turbulent time scale $t(k) \gg \tau_s$, the corresponding relative velocity $w(k) \ll u(k)$, and we approximate $\mathbf{w} \ll \mathbf{u}$. However, the same need not hold when comparing $\nabla \cdot \mathbf{w}$ and $\nabla \cdot \mathbf{u}$ because the latter is resisted by pressure forces. We therefore drop \tilde{w} and $\tilde{\mathcal{D}}$ in favor of \tilde{u} and \mathcal{D} , reducing Equation (A41) to

$$\begin{aligned} \partial_t \bar{n} + \partial_z (\bar{n} \mathcal{D} \partial_z [\ln \bar{\rho} - \ln \bar{n}]) + \partial_z (\bar{n} \bar{w}_z) \\ - \partial_z \left(\overline{t_u u'_z \nabla \cdot \mathbf{w}'} \bar{n} \right) \simeq 0. \end{aligned} \quad (\text{A42})$$

Combining Equations (A34) and (A42), repeating the approxima-

tion that derivatives on fluctuating quantities dominate over derivatives on background quantities, we come at long last to

$$\begin{aligned} \partial_t \bar{n} + \partial_z (\bar{n} \mathcal{D} \partial_z [\ln \bar{\rho} - \ln \bar{n}]) + \partial_z (\bar{n} \bar{w}_z) \\ - \partial_z \left(\frac{\bar{\tau}_s}{\bar{\rho}} \overline{t_u u'_z \nabla^2 p'} \bar{n} \right) \simeq 0. \end{aligned} \quad (\text{A43})$$

Equation (A43) is the general low Mach number turbulent averaged particle fluid continuity equation under standard mean-field decompositions and for common scale-separation assumptions. We next explore its final term and derive the TTD.

A6 Pressure fluctuations in the presence of a temperature gradient

Using Equation (A43) we can define the particle flux F_n in the \hat{e}_z direction:

$$\partial_t \bar{n} + \partial_z (F_n) \simeq 0. \quad (\text{A44})$$

$$F_n \equiv \bar{n} \left(\mathcal{D} \partial_z [\ln \bar{\rho} - \ln \bar{n}] + \bar{w}_z - \frac{\bar{\tau}_s}{\bar{\rho}} \overline{t_u u'_z \nabla^2 p'} \right). \quad (\text{A45})$$

In Equation (A45), the first term on the right-hand side is the diffusive flux, the second the large scale particle drift due to a background pressure gradient. The third term is the source of the so-called turbulent thermal diffusion.

We can use the ideal gas equation of state to write, to first order in fluctuating quantities,

$$\bar{p} = \frac{k_B}{m} \bar{\rho} \bar{T}, \quad (\text{A46})$$

$$p' = \frac{k_B}{m} (\bar{\rho} T' + \rho' \bar{T}), \quad (\text{A47})$$

$$\frac{\bar{\tau}_s}{\bar{\rho}} \overline{t_u u'_z \nabla^2 p'} = \frac{\bar{\tau}_s k_B}{m \bar{\rho}} \overline{t_u u'_z \nabla^2 (\rho' \bar{T} + \bar{\rho} T')} \quad (\text{A48})$$

where m is the mean molecular mass of the gas. The key insight of Elperin et al. (1996) was that the correlation of $u'_z \nabla^2 \rho'$ in Equation (A48) is small because it represents turbulent transport of mass, but the correlation of $u'_z T'$ is large in the presence of a large scale temperature gradient, because it represents the turbulent transport of temperature down a temperature gradient.

We therefore neglect the ρ' component of Equation (A47) and write the equation for turbulent thermal diffusion as:

$$\begin{aligned} -\frac{\bar{\tau}_s}{\bar{\rho}} \overline{t_u u'_z \nabla^2 p'} &\simeq -\frac{\bar{\tau}_s}{\bar{\rho}} \overline{t_u u'_z \nabla^2 \frac{k_B}{m} \bar{\rho} T'} \\ &\simeq -\frac{\bar{\tau}_s k_B}{m} \overline{t_u u'_z \nabla^2 T'} \equiv V_{\text{TTD}}, \end{aligned} \quad (\text{A49})$$

where we have neglected $\nabla^2 \bar{\rho}$ because turbulent length scales are assumed shorter than turbulent ones. In the absence of strong cooling terms, temperature is approximately advected:

$$T' = -C t_u u'_z \partial_z \bar{T}, \quad (\text{A50})$$

for a turbulent transport coefficient C of order unity which depends on the nature of the turbulence (Zilitinkevich et al. 2007). Combining Equations (A49) and (A50) we find

$$\begin{aligned} V_{\text{TTD}} &\simeq C \frac{\bar{\tau}_s k_B}{m} \partial_z \bar{T} \overline{t_u u'_z \nabla^2 t_u u'_z}, \\ &\simeq C \frac{\bar{\tau}_s k_B \bar{T}}{m} \partial_z \ln \bar{T} \overline{t_u u'_z \nabla^2 t_u u'_z}, \end{aligned} \quad (\text{A51})$$

where we have again used scale separation to neglect derivatives on non-turbulent gradients.

For Kolmogorov turbulence we have

$$t_u = 2t_0 \left(\frac{k}{k_0} \right)^{-2/3}, \quad (\text{A52})$$

$$|u'| = u_0 \left(\frac{k}{k_0} \right)^{-1/3}. \quad (\text{A53})$$

Accordingly, we can calculate \mathcal{D} by integrating over the turbulent cascade:

$$\mathcal{D} = \overline{t_u u'_z} = \int_{k_0}^{k_\eta} B 2t_0 \left(\frac{k}{k_0} \right)^{-2/3} u_0 \left(\frac{k}{k_0} \right)^{-2/3} \frac{dk}{k}. \quad (\text{A54})$$

For isotropic turbulence Kolmogorov turbulence we have $B = 2/9$, and the dissipation wavenumber

$$k_\eta = Re^{3/4} k_0, \quad (\text{A55})$$

where Re is the Reynolds number of the turbulence. For astrophysical turbulence, we generally have $Re \gg 1$ and so

$$\mathcal{D} = \frac{t_0 u_0^2}{3}. \quad (\text{A56})$$

Replacing $\nabla^2 \rightarrow k^2$ we can also calculate

$$\begin{aligned} \overline{t_u u'_z \nabla^2 t_u u'_z} &= \int_{k_0}^{k_1} B \left[4t_0^2 \left(\frac{k}{k_0} \right)^{-4/3} \right] \left[u_0^2 \left(\frac{k}{k_0} \right)^{-2/3} \right] k^2 \frac{dk}{k}, \\ &= -\frac{8}{9} \int_{k_0}^{k_1} \frac{dk}{k} = -\frac{8}{9} \ln(k_1/k_0), \end{aligned} \quad (\text{A57})$$

where k_1 is the limiting wave number. We have assumed that $\tau_s < t_u$, which imposes

$$\frac{k_1}{k_0} < \left(\frac{1}{St} \right)^{3/2}, \quad (\text{A58})$$

where

$$St \equiv \frac{\tau_s}{2t_0} \quad (\text{A59})$$

is the Stokes number defined with respect to the integral scale of the turbulence. In astrophysical contexts the Reynolds number Re is typically very large, so in practice Equation (A58) is the controlling factor in setting the upper limit in the integral in Equation (A57), rather than the limit

$$k_1 = k_\eta = Re^{3/4} k_0 \quad (\text{A60})$$

set by the dissipation scale of the turbulence. Further, V_{TTD} depends linearly on St so its effects will be negligible unless St is large enough that Equation (A58) is indeed the controlling limit.

In much of the existing literature, Equation (A55) is the limit used, and in the cases where Equation (A58) is invoked, it is done so in the Stokes drag regime. Many cases of astrophysical interest are in the Epstein drag regime so we proceed using the more general formulation in Equation (A58), resulting in the equations for the particle flux:

$$F_n = \bar{n} (\mathcal{D} \partial_z [\ln \bar{\rho} - \ln \bar{n}] + \bar{w}_z + V_{\text{TTD}}). \quad (\text{A61})$$

$$V_{\text{TTD}} = -\frac{4}{3} C \frac{\bar{\tau}_s k_B \bar{T}}{m} \ln St^{-1} \partial_z \ln \bar{T}. \quad (\text{A62})$$

A7 Velocity limits

An interesting feature of Equation (A62) is that the turbulent velocity scale has cancelled out, and for an arbitrarily large $\partial_z \ln \bar{T}$,

we would have $V_{\text{TTD}} > u_0$, which would be absurd. Returning to Equation (A51), note that

$$\frac{n'_{T'}}{\bar{n}} = C \frac{\bar{\tau}_s k_B \bar{T}}{m} \partial_z \ln \bar{T} t_u \nabla^2 t_u u'_z \quad (\text{A63})$$

is the fractional particle number density fluctuation due to the temperature fluctuations. We have assumed that the turbulent fluctuations are small enough that they can be treated to first order, so we require $n'_{T'} \ll \bar{n}$, which in turn constrains $V_{\text{TTD}} \ll u_0$. For Kolmogorov turbulence, the right hand side of Equation (A63) is proportional to

$$t_u^2 \nabla^2 u'_z \propto k^{1/3}, \quad (\text{A64})$$

and so the requirement that

$$\frac{n'_{T'}}{\bar{n}} = C \frac{\bar{\tau}_s k_B \bar{T}}{m} \partial_z \ln \bar{T} t_u \nabla^2 t_u u'_z \ll 1 \quad (\text{A65})$$

is a requirement on both $\partial_z \ln \bar{T}$ and on the upper limit k_1/k_0 for the integral in Equation (A57). Throughout this paper we assume that $\partial_z \ln \bar{T}$ is sufficiently small that Equation (A62) can be used. When that is not the case, Equation (A62) overestimates V_{TTD} , but in that case the concentration of particles invoked by TTD is large enough to be non-negligible on its own terms.

A8 Quasi-isobaric case

In the limit where $\partial_z \bar{p} = 0$, we have

$$\partial_z \ln \bar{p} = -\partial_z \ln \bar{T}, \quad (\text{A66})$$

and we can write Equation (A45) as

$$\begin{aligned} F_n &= \bar{n} \left(-\mathcal{D} \partial_z [\ln \bar{T} + \ln \bar{n}] - \frac{4}{3} C \bar{\tau}_s \frac{k_B \bar{T}}{m} \ln \text{St}^{-1} \partial_z \ln \bar{T} \right) \\ &= -\mathcal{D} \bar{n} \left(\left[1 + \frac{4C}{3\mathcal{D}} \bar{\tau}_s \frac{k_B \bar{T}}{m} \ln \text{St}^{-1} \right] \partial_z \ln \bar{T} + \partial_z \ln \bar{n} \right). \end{aligned} \quad (\text{A67})$$

Defining

$$\alpha \equiv 1 + \frac{4C}{3\mathcal{D}} \bar{\tau}_s \frac{k_B \bar{T}}{m} \ln \text{St}^{-1}, \quad (\text{A68})$$

we see that the steady state solution is

$$\bar{n} \propto \bar{T}^{-\alpha}, \quad (\text{A69})$$

where \bar{n} and \bar{T} are observables in both laboratory experiments and the Earth's atmosphere, allowing α to be evaluated. Values of $\alpha > 2$ have been found in experiments and $\alpha \gtrsim 20$ in measurements of aerosols in the Earth's tropopause. Under these definitions,

$$V_{\text{TTD}} = -(\alpha - 1) \mathcal{D} \partial_z \ln \bar{T}. \quad (\text{A70})$$

A9 Falsifying rapid pressure equilibration

It might seem natural to assume that low Mach number turbulence experiences rapid pressure equilibration, and therefore that p' is set by the constraint that vertically traveling parcels of gas rapidly expand or contract to maintain pressure equilibration. However, as we show here, it that were the case then particle transport would be negligible, which is incompatible with the results of laboratory investigations of the TTD. In the isobaric case, rapid equilibration would imply $p' = 0$ in the absence of thermal equilibration, which has been ruled out by the experiments which found $\alpha > 1$.

Assuming instead perfect thermal equilibration results in the following approximations for Equations (A1) and (A3):

$$\partial_t \rho \simeq 0 \simeq -u'_z \partial_z \bar{p} - \bar{\rho} \nabla \cdot \mathbf{u}', \quad (\text{A71})$$

$$\partial_t \nabla \cdot \mathbf{u}' \simeq -\frac{1}{\bar{\rho}} \nabla^2 p'. \quad (\text{A72})$$

Under the assumption of small turbulent correlation times we can also estimate

$$\nabla \cdot \mathbf{u}' \simeq t_u \partial_t \nabla \cdot \mathbf{u}'. \quad (\text{A73})$$

Inserting Equation (A72) into Equation (A73) we find

$$\nabla \cdot \mathbf{u}' \simeq -\frac{t_u}{\bar{\rho}} \nabla^2 p'. \quad (\text{A74})$$

Combining Equations (A71) and (A74), we arrive at

$$\nabla^2 p' \simeq \frac{u'_z}{t_u} \partial_z \bar{p}, \quad (\text{A75})$$

which when inserted into Equation (A45) would imply

$$V_{\text{TTD}} \simeq -\frac{\bar{\tau}_s}{\bar{\rho}} \overline{t_u u'_z \frac{u'_z}{t_u} \partial_z \bar{p}} = -\frac{\bar{\tau}_s \overline{u_z'^2}}{\bar{\rho}} \frac{\partial_z \bar{p}}{\bar{\rho}} = -\frac{\bar{\tau}_s u_0^2}{3} \partial_z \ln \bar{p}, \quad (\text{A76})$$

and in the case of Kolmogorov turbulence with zero large scale pressure gradients this reduces to

$$V_{\text{TTD}} \simeq -2\text{St} \mathcal{D} \partial_z \bar{p} = 2\text{St} \mathcal{D} \partial_z \bar{T}, \quad (\text{A77})$$

which has the opposite sign as the prediction of turbulent thermal diffusion. Thus this approximation would predict $\alpha - 1 < 0$ which has been ruled out by observation and experiment.

We could also assume that p' is controlled by the turbulent ram pressure $\bar{\rho} |u'|^2$. In the absence of large scale gradients in the gas, symmetry implies that the ram pressure fluctuations cannot correlate with u'_z in Equation (A45). However, in the presence of a temperature gradient we can postulate

$$|p'| \sim |\bar{\rho} u_z'^2 k^{-1} \partial_z \ln \bar{T}|, \quad (\text{A78})$$

where the $k^{-1} \ln \bar{T}$ term provides the required isotropy breaking for a correlation to exist. In the case of Kolmogorov turbulence this reduces to

$$|V_{\text{TTD}}| = |4\text{St} \mathcal{D} \partial_z \bar{T}| \ll |\mathcal{D} \partial_z \bar{T}|, \quad (\text{A79})$$

and so would predict

$$|\alpha - 1| \ll 1, \quad (\text{A80})$$

which also ruled out by experiment and observation.